VOL. 11, NO. 14, JULY 2016 ISSN 1819-6608
ARPN Journal of Engineering and Applied Sciences

www.arpnjournals.com

COMPUTER AIDED DIAGNOSIS (CAD) TOOL FOR THE ANALYSIS OF CALCANEOFIBULAR LIGAMENT USING ULTRASONOGRAPHIC IMAGES

Vedpal Singh[1], Irraivan Elamvazuthi[1], Varun Jeoti[1], John George[2] and Dileep Kumar[1]
[1]Universiti Teknologi Petronas, Bandar Seri Iskandar, Perak Darul Ridzuan, Malaysia
[2]Research Imaging Centre, University of Malaya, Malaysia
E-Mail: irraivan_elamvazuthi@petronas.com.my

ABSTRACT

Ultrasound imaging is a cost-effective diagnostic tool to imagine the internal organisms of human beings that used routinely in the diagnosis of a number of diseases related to ligament, tendon, bone, blood flow estimation, obstetrics, etc. However, ultrasound imaging has limitations such as homogenous intensity regions, homogeneous textures, low contrast regions, enhancement artefact, limited view visualization and inaccurate qualitative/quantitative estimation. To overcome all these investigated problems, this research developed a Computer Aided Diagnosis (CAD) system that helps in efficient segmentation and Three Dimensional (3D) reconstruction of calcaneofibular ligament to enhance the diagnosis. The developed CAD system would help in the achievement of enhanced segmentation results, 3D reconstruction results and statistical analysis of the injured calcaneofibular ligament. Moreover, performance of the developed CAD system is analyzed based on the obtained results, which are indicates the improved performance with more than 92% accurate segmentation and precisely determined 3D measurements such as volume, thickness and roughness. In addition, this research opens new research dimensions for efficient musculoskeletal ultrasound modelling that makes it useful in clinical settings with accurate and cost effective diagnosis of calcaneofibular ligament injuries.

Keywords: ultrasound imaging, CAD system, segmentation, 3D reconstruction.

INTRODUCTION

Human beings are increasingly surrounded by injuries and abnormalities in various anatomical parts specifically, ankle ligaments. Ankle ligament is a short band of tough fibrous connective tissues made by long, strongly collagen fibers. Generally, ligament connects bones to the other bone for making a joint (Freeman, 1965; Ligaments, 1994). Although ligaments by nature are very strong and rigid, but sometimes strains, inflammation and sudden forces may be the cause of injuries such as tear, bruise, rupture etc. (Bland-Sutton, 1897). Ligament injuries and abnormalities are frequently happened in the association of joint debris and diffuse bone marrow edema. Indeed, there is often coexistence of these features, so it is difficult to determine, which may have occurred first in the ankle patients (Tegner and Lysholm, 1985). Basically, ankle is a collection of four kinds of ligaments such as anterior talofibular ligament, posterior talofibular ligament, calcaneofibular ligament and deltoid ligament (Singh *et al*., 2014; Tegner and Lysholm, 1985). Ankle ligaments are prone to injuries due to sports, accidents, high ankle sprains and inflammation (Flegel, 2013; Singh *et al*., 2015).

However, sports are the important recreational and professional activity that is growing worldwide. Increasingly, sports activities may be the big causes of injuries. The most common cause of injuries in ankle ligaments is the inversion of foot (Muschol *et al*., 2005; Tegner and Lysholm, 1985) that frequently damage the Calcaneofibular Ligament (CFL) ligament (Smith and Reischl, 1986). A total rupture involves the injuries in anterior talofibular and posterior talofibular ligaments as well (van Dijk, 1994). Another kind of injury is the eversion that leads to damage in deltoid ligaments during sports (Broström, 1966). In earlier studies, it was reported that 20% of registered sports professionals sustain injuries every year. In addition, it was estimated that 14% of the sports injuries are belongs to ankle and out of these 80% injuries related to ligaments (Kannus and Renström, 1991; Muschol *et al*., 2005; Trevino *et al*., 1994). Thus, ankle ligament was found to be the most prevalent injury body part (Eisenhart *et al*., 2003; Singh *et al*., 2015; Tegner and Lysholm, 1985).

Problem formulation

As shown in Figure-1, CFL ligament represents the random structure and shape that turn to wrong interpretation. In particular, when ultrasound images of CFL exhibit homogeneous contrast (indicated by red rectangle and green arrow) and homogeneous texture (specified by the green color arbitrary shapes) compared to surrounded tissues as shown in Figure-1a and Figure-1b, respectively. In addition, low contrast in CFL region makes it difficult to interpret the defects in injured CFL is indicated by the red color circles in Figure-1c. Figure-1d is focused on the enhancement artefact that may be the cause of enhancement in contrast in CFL region presented by the red color arrows. Due to these existing issues of CFL ultrasound images, direct interpretation and visualisation of defects associated with injured CFL is not recommended that requires involvement of computation method to segment the CFL region from ultrasound images that lead to enhanced diagnosis to start the better treatment.

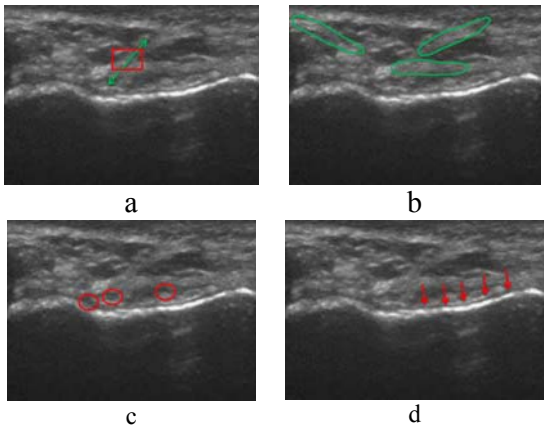

Figure-1. Challnges of the CFL ligament ultrasound image.

Due to the challenges mentioned above, segmentation of CFL from ultrasound images remains a challenging task that has not been studied at wide, but it can lead to disease diagnosis in therapy and image guided interventions. To overcome this problem, this research used pre-processing, optimization and ROI (Region of Interest) extraction and morphological operation in the development of the CAD system. This unique association would leads to enhanced diagnosis of CFL. Furthermore, for more enhancements 3D reconstruction is performed on the segmented results through the integration of image registration method, enhanced marching cube method, patching and rendering methods to recover the problems of 2D ultrasound imaging such as limited view visualization and inaccurate qualitative/quantitative estimation. Therefore, this research uses the integration of segmentation and 3D reconstruction approaches in the development of CAD system.

MATERIAL AND METHODS

Image dataset

A total of 450 ultrasound images of CFL from the 9 patients were included in this study. There are 4 normal and 5 abnormal patients, whose ages ranged from 23-50 years were selected to acquire ultrasound images of CFL ligament. For ultrasound scanning, linear probe (5-13 MHz) of iU22 Philips colour ultrasound system is used to create video of 3-5 seconds (1 second video provides 30 image frames) for each scan. All obtained images are stored in hard disk and transferred to personal computer for further processing. Institutional medical ethics approval was obtained prior to the study. Subjects were informed about the study protocol and consent form is obtained from all the subjects.

Experimental methods

The developed CAD system is tested on the acquired datasets using MATLAB (MathWorks, Inc., MA) (Gonzalez *et al*., 2004; Guide, 1998). In acquired datasets, a closer examine of 2D images shows that first 2 and last 2 image frames exhibits inherently low quality as compared to other images in single acquisition. Thus, 4 images in each of single scan data were excluded to preserve the maximum accuracy during post-processing. The total images that represent the CFL ligament at different contrast, locations and patterns are processed using the developed CAD system. In addition, performance evaluation of the developed CAD system is carried out on the basis of obtained results to validate this research.

THE DEVELOPED CAD SYSTEM

This section demonstrates the process flow of the developed CAD system that comprises of data acquisition, segmentation, 3D reconstruction and volume calculation as shown in Figure-2. The functionalities of the segmentation include data acquisition using readily available device, pre-processing, optimization and ROI extraction, morphological operations that produced the accurate segmented results. In addition, 3D ultrasound reconstruction involved four steps such as image registration, enhanced marching cube method to reconstruct a 3D mesh, which is followed by patching and rendering to reconstruct the accurate 3D image. The reconstructed 3D model is used for volume calculation.

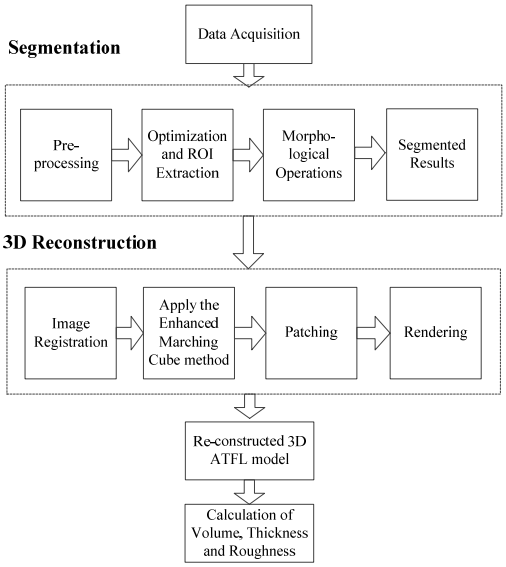

Figure-2. Process flow of the developed CAD system.

For better understanding of the developed CAD system, the methodology is explained in Table-1.

Table-1. Pseudocode of the developed CAD system.

if acquired data is *accurate*
Go for *pre – processing*
else
Collect data again
end
if pre – processing is successful
Optimize the images through *DPSO algorithm*
else
Apply *pre – processing*
end
if Optimization is *accurate*
Apply *curve evolution* using Chan-Vese method for *ROI extraction*
else
Change the variable settings of the *DPSO algorithm*
end
while (extracted *ROI* image is not smooth enough)
Apply the *morphological operation* until sufficient smoothing
end
Multiply the smoothed *ROI* to original image
Collect all the smoothed segmented images
if orientation of all segmented images is *accurate*
Go for *3D* reconstruction by the use of *enhanced marching cube method*
else
Apply *image registration* method to adjust the *orientation* of segmented images
end
Patching is performed on the obtained *3D* mesh
Patched 3D mesh is smoothed by the *Rendering method* for better visualization
if reconstructed *3D* model is *accurate*
Calculate *Volume*, *Thickness* and *Roughness*
end
else
Repeat the *3D* reconstruction process
end

where, *DPSO algorithm* is the Darwinian Particle Swarm Optimization algorithm

RESULTS AND DISCUSSIONS

The Graphical User Interface (GUI) of the developed CAD system is shown in Figure-3 that comprises of various functions such as main information, segmentation, 3D reconstruction, volume calculation, statistical analysis, input database, repository of segmented results and 3D models and contact details, which are indicated by the red colour arrows.

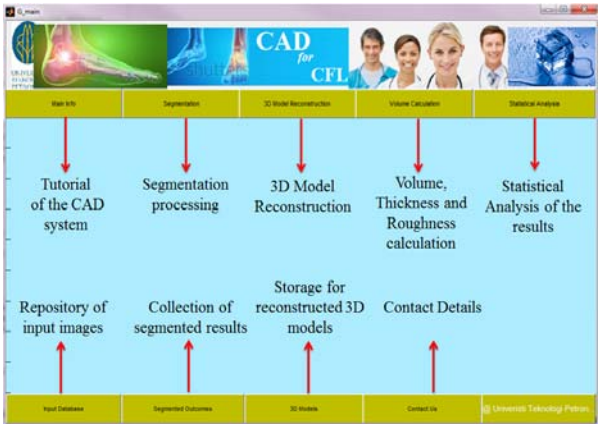

Figure-3. GUI of the developed CAD system.

As illustrated in Figure-3, the developed CAD system produced the efficient segmented results that would help in enhanced diagnosis of CFL injuries. In addition, it can produce the better 3D results due to the use of enhanced methods (e.g. enhanced active contour and enhanced marching cube methods).

Segmentation of CFL ligament through developed CAD system

The developed CAD system is tested on 9 patient's database and it produced the enhanced results. However, here only one sample image is used to demonstrate the complete process flow of segmentation with the corresponding results as depicted in Figure-4.

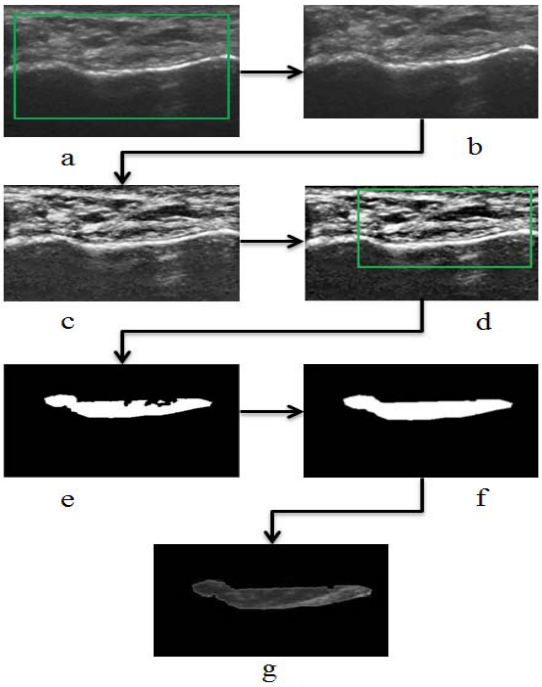

Figure-4. The developed CAD segmentation processing.

Initially, the input image is pre-processed such as ROI initialization (see Figure-4a and-4b) and contrast enhancement as shown in Figure-4c, in which the CFL region is more clearly visualized than the input image. The pre-processed results are further used in optimization and ROI extraction as illustrated in Figure-4d that try to extract the CFL region more accurately through the energy minimization and curve evolution process. The extracted CFL region is presented in Figure-4e, but its boundaries are not smooth. To make it smooth, morphological operation is applied that produced the results, which is shown in Figure-4f, whose boundaries are clearer. Furthermore, the smoothed image is overlaid on the input image to get the better visualization, which is presented in Figure-4g.

3D reconstruction of CFL ligament through developed CAD system

The obtained segmented results are further used in 3D reconstruction of CFL ligament for better diagnosis. In this study, only 50 images per patient were used in the experiments. For 3D reconstruction, this research initially used the image registration algorithm to adjust the orientation of segmented images with respect to one image as described in Table-2.

Table-2. 3D reconstruction of CFL ligament.

Data-sets	Image Registration	3D Reconstruction by the developed CAD system
1	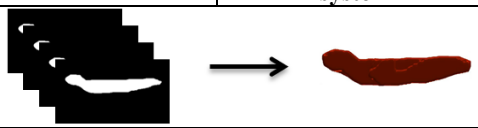	
2	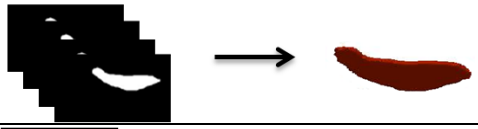	
3	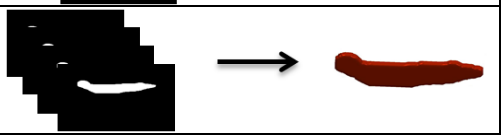	

The accurately oriented images are further processed by the enhanced marching cube method to design the 3D mesh model. The obtained 3D mesh is efficiently converted into the 3D model by the patching operation, which is not smooth enough. Furthermore, reconstructed 3D model is smoothed by the rendering operation that would be the 3D image as presented in Table-2. It should be noted that this paper illustrated the 3D results of only three datasets out of nine to reduced the complexity for better understanding.

Performance evaluation based on image features

To evaluate the performance of the developed CAD system, this research used some parameters such as Peak Signal to Noise Ratio (PSNR), Root Mean Square Error (RMSE), Standard Deviation (SD), Universal Image Quality Index (UIQI), Mean Absolute Error (MAE), Normalized Absolute Error (NAE) and Normalized Cross Correlation (NCC) that are illustrated in Table-3.

Table-3. Statistical analysis of the developed CAD system for ankle CFL ligament.

	Min.	Max.	Average
PSNR	30.20	30.29	30.25
RMSE	7.79	7.87	7.82
SD	42.62	43.91	42.95
UIQI	0.87	0.80	0.79
MAE	16.90	17.16	17.04
NAE	1.01	1.06	1.04
NCC	0.20	0.27	0.22

The Table-3 demonstrated the quantitative analysis of the developed CAD system that provides information regarding the noise ratio, image energy, error rate and correlation between the original and resultant images. The PSNR ranges from minimum 30.20 to maximum 30.29 with the average estimation of 30.25. The

RMSE values varies minimum 7.79 to maximun 7.87 and mean is 7.82. The obtained PSNR and RMSE values are indicating the better signal strength and lowest error ratio of the segmented images. Likewise, SD ranges from 42.62 to 43.91 with 42.95 average value that shows variance of resultant images with respect to the input images. In order to evaluate the quality of the segmented results, this research used the UIQI metrics that ranges from minimum 0.57 to maximum 0.80 with the 0.59 mean value that are depicted the good quality of the obtained results. In addition, parameter MAE is varied from 16.90 to 17.16 with the average 17.04 value that indicated the error rate of the obtained results. The NAE ranges from 1.01 to 1.06 and the average estimated value is 1.04. Furthermore, to identify the similarity correlation of segmented images based on the input image; this research used the NCC measurement metrics that ranges from 0.20 to 0.27 and average correlation is 0.22. Therefore, obtained results are indicating the better performance of the developed CAD system.

Performance evaluation against the expert's segmentation

After the segmentation performed by the developed method, three experts are requested to do the manual segmentation. The results obtained from the developed CAD system are compared with manual segmented results by the use of sensitivity, specificity and accuracy metrics that are demonstrated in Table-4. This paper demonstrated the results on the basis of 24 images from the diverse subjects for better understanding and reduced the complexity.

Table-4. Performance evaluation based on sensitivity, specificity and accuracy measurements.

Image ID	Sensitivity	Specificity	Accuracy
1	81.28	96.04	93.79
2	80.49	96.13	93.74
3	79.51	96.14	93.60
4	84.23	96.24	94.51
5	82.03	96.04	94.00
6	85.94	95.78	94.43
7	81.83	96.34	94.15
8	82.75	96.27	94.28
9	81.09	96.73	94.29
10	83.59	96.51	94.62
11	83.64	96.62	94.70
12	84.71	96.62	94.85
13	83.15	97.00	94.84
14	80.93	96.66	94.23
15	82.25	96.65	94.47
16	75.28	97.01	93.39
17	74.34	96.83	93.07
18	73.69	96.87	92.98
19	76.89	96.74	93.62
20	76.39	97.30	93.81
21	79.23	96.39	93.87
22	82.29	97.10	94.85
23	78.53	97.40	94.36
24	83.51	96.29	94.52

As presented in Table-4, sensitivity ranges from 73.69% to 85.94%. Similarly, specificity varies from minimum 95.78% to maximum 97.40%. The obtained results of accuracy metrics are lies between 92.98% - 94.85%. Thus, on the basis of all obtained outcomes, the average sensitivity, specificity and accuracy of the developed method are 80.73%, 96.57% and 94.12%, respectively. Therefore, obtained outcomes are indicating the better performance of the developed CAD system that produced more accurate results (accuracy is more than 92%), which represented the promising behavior of the developed CAD system.

Volume, thickness and roughness estimation through developed CAD system

For more validation, the developed CAD system is implemented on 9 patients and determined the volume, thickness and roughness of the reconstructed 3D models that are explained in Table-5.

Table-5. Volume, thickness and roughness calculation.

Dataset	Volume	Thickness	Roughness
1	1006.14 mm^3	2.12 mm	0.108 mm
2	990.57 mm^3	2.03 mm	0.110 mm
3	1103.76 mm^3	2.09 mm	0.152 mm
4	1089.23 mm^3	2.19 mm	0.134 mm
5	1045.59 mm^3	2.07 mm	0.105 mm
6	1208.10 mm^3	1.98 mm	0.113 mm
7	1186.92 mm^3	2.22 mm	0.109 mm
8	1076.12 mm^3	2.01 mm	0.114 mm
9	1139.98 mm^3	1.87 mm	0.116 mm

As demonstrated in Table-5, the estimated volume ranges from minimum 990.57 mm^3 to maximum 1208.1 mm^3. Similarly, thickness varies from minimum 1.87 mm to maximum 2.22 mm. Furthermore, surface roughness of the reconstructed 3D model is minimum 0.105 mm and maximum is 0.152 mm, which indicated the smoothness of the obtained results.

In this study, performance of the developed CAD system is analyzed based on the visual inspection of the

obtained results by the three expert radiologists. In addition, some key imaging metrics such as PSNR, RMSE, SD, UIQI, MAE, NAE and NCC are used to estimate the performance of the developed CAD system with respect to the image quality. However, sensitivity, specificity and accuracy metrics are also calculated against the ground truths, which are producing the good results with more than 92% accuracy. Moreover, in order to validate this research, this study determined the volume, thickness and roughness of the reconstructed 3D models of the acquired 9 datasets. Therefore, obtained results are indicated the promising performance of the developed CAD system that would lead to accurate and enhanced diagnosis of CFL ligament.

CONCLUSIONS

This research developed a novel CAD system for efficient diagnosis of CFL ligament injuries through segmentation and 3D reconstruction based on 2D ultrasound images. The developed CAD system uses the integration of pre-processing, optimization and ROI extraction, morphological operation, image registration, enhanced marching cube method, patching and rendering methods to overcome the investigated problems of CFL ultrasound images. Moreover, performance of the developed CAD system is evaluated based on sensitivity, specificity and accuracy metrics, which are indicated the improved performance. In addition, the developed CAD system is capable to produce the better quality 3D image models of CFL with accurate geometrical measurements such as volume, thickness and roughness. Therefore, obtained results are signifying that the developed CAD system is well suited for the diagnosis of CFL ligament. In addition, the developed CAD system has opened new entrances for clinicians, radiologists, orthopedist, rheumatologists and sports physician to diagnose the injuries of CFL. In future, the developed CAD system could be extended to other musculoskeletal anatomical parts with further refinements.

ACKNOWLEDGEMENT

The authors would like to thank UTP, Malaysia for their assistance and Ministry of Education (MOE) for sponsoring the project under grant entitled ‘Formulation of Mathematical Model for 3-D Reconstruction of Ultrasound Images of MSK Disorders’ (Grant no. 0153AB-I55).

REFERENCES

Bland-Sutton, J. 1897. "Ligaments; Their Nature and Morphology," Lewis.

Broström, L. 1966. Sprained ankles. V. Treatment and prognosis in recent ligament ruptures. Acta chirurgica Scandinavica 132, 537-550.

Eisenhart, A. W., Gaeta, T. J., and Yens, D. P. 2003. Osteopathic manipulative treatment in the emergency department for patients with acute ankle injuries. JAOA: Journal of the American Osteopathic Association 103, 417-421.

Flegel, M. 2013. "Sport First Aid, 5E," Human Kinetics.

Freeman, M. 1965. Instability of the foot affer injuries to the lateral ligament of the ankle. Journal of Bone & Joint Surgery, British Volume 47, 669-677.

Gonzalez, R. C., Woods, R. E., and Eddins, S. L. 2004. "Digital image processing using MATLAB," Pearson Education India.

Guide, M. U. s. 1998. The MathWorks Inc. Natick, MA 4, 382.

Kannus, P., and Renström, P. 1991. Treatment for acute tears of the lateral ligaments of the ankle. Operation, cast, or early controlled mobilization. The Journal of Bone & Joint Surgery 73, 305-312.

Ligaments, L. A. 1994. Current methods for the evaluation of ankle ligament injuries.

Muschol, M., Müller, I., Petersen, W., and Hassenpflug, J. (2005). Symptomatic calcification of the medial collateral ligament of the knee joint: a report about five cases. Knee Surgery, Sports Traumatology, Arthroscopy 13, 598-602.

Singh, V., Elamvazuthi, I., Jeoti, V., and George, J. 2014. 3D reconstruction of ATFL ligament using ultrasound images. In "Intelligent and Advanced Systems (ICIAS), 2014 5th International Conference on", pp. 1-5. IEEE.

Singh, V., Elamvazuthi, I., Jeoti, V., and George, J. 2015. Automatic Ultrasound Image Segmentation Framework Based on Darwinian Particle Swarm Optimization. In "Proceedings of the 18th Asia Pacific Symposium on Intelligent and Evolutionary Systems, Volume 1", pp. 225-236. Springer.

Smith, R. W., and Reischl, S. F. 1986. Treatment of ankle sprains in young athletes. The American journal of sports medicine 14, 465-471.

Tegner, Y., and Lysholm, J. 1985. Rating systems in the evaluation of knee ligament injuries. Clinical orthopaedics and related research 198, 42-49.

Trevino, S. G., Davis, P., and Hecht, P. J. 1994. Management of acute and chronic lateral ligament injuries of the ankle. The Orthopedic clinics of North America 25, 1-16.

Van Dijk, C. N. 1994. "On diagnostic strategies in patients with severe ankle sprain," Rodopi.